Inorg. Chem. **2005**, *44*, 6265–6276

One-Dimensional and Two-Dimensional Coordination Polymers from Self-Assembling of Trinuclear Triangular Cu(II) Secondary Building Units

Maurizio Casarin,[†] Carlo Corvaja,[†] Corrado Di Nicola,[‡] Daniele Falcomer,[†] Lorenzo Franco,[†] Magda Monari,*[,§] Luciano Pandolfo,*[,†] Claudio Pettinari,*[,‡] and Fabio Piccinelli[§]

Department of Chemical Sciences, University of Padova, Via Marzolo, 1, I-35131 Padova, Italy, Department of Chemical Sciences, Via S. Agostino, 1, University of Camerino, I-62032 Camerino (MC), Italy, and Department of Chemistry "G. Ciamician", University of Bologna, Via Selmi, 2, I-40126 Bologna, Italy

Received May 2, 2005

The reactions of pyrazole (Hpz) with some copper(II) carboxylates in the presence of water yield trinuclear copper derivatives characterized by the triangular core $[Cu_3(\mu_3\text{-}OH)(\mu\text{-}pz)_3(RCOO)_2]$ (R = H, C_2H_5, C_3H_7). Copper(II) formate gives $[Cu_3(\mu_3\text{-}OH)(\mu\text{-}pz)_3(HCOO)_2(Hpz)_2]$ (**1**), whereas copper propionate and butyrate afford $[Cu_3(\mu_3\text{-}OH)(\mu\text{-}pz)_3(C_2H_5COO)_2(EtOH)]$ (**2**) and $[Cu_3(\mu_3\text{-}OH)(\mu\text{-}pz)_3(C_3H_7COO)_2(MeOH)(H_2O)]$ (**3**), respectively, both containing solvent molecules coordinated to copper atoms. Magnetic susceptibilities are consistent with a single unpaired electron for each trinuclear unit of **1**–**3**, and EPR measurements indicate that higher spin states, generated by exchange coupling between copper atoms, may be populated at room temperature. Density-functional calculations provide the description of the electronic structures of **1**–**3**, allowing, at the same time, the assignment of their UV–vis absorption spectra. X-ray molecular structure determinations show that triangular trinuclear units of **1** are connected to each other through single formate bridges, forming one-dimensional (1D) zigzag coordination polymers, whereas in **2** and **3**, two oxygen atoms of two carboxylate ions doubly bridge two copper atoms of different triangles, thus generating hexanuclear units. Moreover, in **2**, two other propionate ions link together two hexanuclear units yielding a 12-membered cycle and giving rise to 1D coordination polymers. The supramolecular assemblies of **1**–**3** are compared to that of the previously reported trinuclear triangular copper(II) derivative $[Cu_3(\mu_3\text{-}OH)(\mu\text{-}pz)_3(CH_3COO)_2(Hpz)]$ (**A**), where a two-dimensional (2D) coordination polymer is present. The reactions of 3,5-dimethylpyrazole (Hpz*) with copper(II) carboxylates in the same conditions yield 1:2 $Cu(RCOO)_2$/Hpz* adducts.

Introduction

Di- and polynuclear copper(II) complexes are the focus of a large number of recent papers, mainly due, on one hand, to the fact that copper is an essential bioelement responsible for numerous catalytic processes in living organisms where it is often present in di- or trinuclear assemblies[1] and, on the other hand, to the possibility provided by copper(II) polynuclear complexes of exploration of magneto-structural correlations resulting from the mutual interaction among metal centers.[2]

The coordinative flexibility of copper(II) ions coupled with the possible presence of carboxylates, which show a large variety of coordination modes (the most frequently observed cases are sketched in Chart 1a−g), can lead to the formation of different assemblies, spanning from mononuclear complexes to supramolecular coordination polymers or metal−organic frameworks (MOFs).[3]

* To whom correspondence should be addressed. E-mail: magda.monari@unibo.it (M.M.), luciano.pandolfo@unipd.it (L.P.), claudio.pettinari@unicam.it (C.P.). Phone: +39 051 2099559 (M.M.), +39 049 8275157 (L.P.), +39 0737 402234 (C.P.). Fax: +39 051 2099456 (M.M.), +39 049 8275161 (L.P.), +39 0737 637345 (C.P.).

[†] University of Padova.

[‡] University of Camerino.

[§] University of Bologna.

(1) (a) Solomon, E. I.; Sundaram, U. M.; Machonkin, T. E. *Chem. Rev.* **1996**, *96*, 2563. (b) Kaim, W.; Rall, J. *Angew. Chem., Int. Ed.* **1996**, *35*, 43. (c) Holm, R. H.; Kennepohl, P.; Solomon, E. I. *Chem. Rev.* **1996**, *96*, 2239.

(2) (a) Kahn, O. *Chem. Phys. Lett.* **1997**, *265*, 109. (b) Ferrer, S.; Haasnoot, J. G.; Reedijk, J.; Muller, E.; Biagini Cingi, M.; Lanfranchi, M.; Manotti Lanfredi, A. M.; Ribas, J. *Inorg. Chem.* **2000**, *39*, 1859. (c) Gutierrez, L.; Alzuet, G.; Real, J. A.; Cano, J.; Borrás, J.; Castiñeiras, A. *Inorg. Chem.* **2000**, *39*, 3608. (d) Ferrer, S.; Lloret, F.; Bertomeu, I.; Alzuet, G.; Borrás, J.; Garcia-Granda, S.; Liu-Gonzales, M.; Haasnoot, J. G. *Inorg. Chem.* **2002**, *41*, 5821.

10.1021/ic050678l CCC: $30.25
Published on Web 08/06/2005

Chart 1

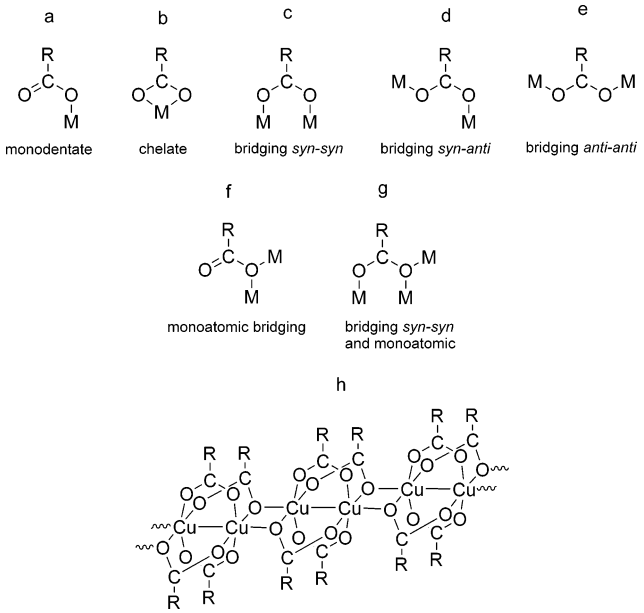

In crystalline MOFs, it is often possible to identify recurring structural motifs, often defined as secondary building units (SBUs),[3] formed by metal cation(s), ligands, and anion(s) (the primary building units). These SBUs (mono- or polynuclear clusters) self-assemble to form one-dimensional (1D), two-dimensional (2D), or three-dimensional (3D) MOFs, and one may look at them as a sort of monomeric unit. For example, this happens in several polymeric copper(II) carboxylates in which the dinuclear *paddlewheel* SBUs $[Cu_2(carboxylate)_4]$ assemble in 1D coordination polymers (Chart 1h). Other types of SBUs and different assembling modes are known, and it is of paramount interest to study the factors determining their formation and assembly in supramolecular structures. Trinuclear triangular metal clusters are potentially interesting SBUs, and even if a relatively large number of naturally occurring[1,4] and synthesized[2b,d,5] trinuclear triangular copper(II) or mixed-valence systems have been reported and characterized, no relevant studies and information concerning their possible supramolecular assemblies are present in the literature.

As part of an ongoing research project dealing with the study of the reactivity of copper(II) carboxylates with azoles,[6]

Scheme 1

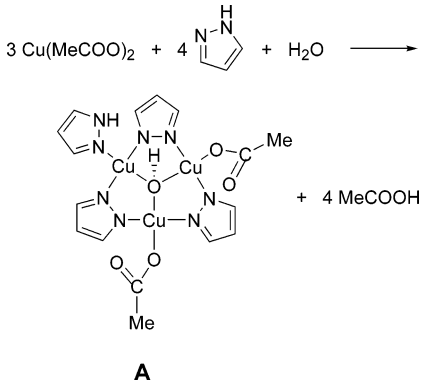

we have recently reported that simple mixing in water or ethanol of pyrazole (Hpz) and hydrated copper(II) acetate leads to spontaneous deprotonation of both water and Hpz, as well as to the rapid and quantitative formation of the trinuclear triangular μ_3-OH capped derivative, $[Cu_3(\mu_3\text{-OH})(\mu\text{-pz})_3(MeCOO)_2(Hpz)]$ (**A**), as shown in Scheme 1.[7]

Trinuclear triangular μ_3-OH capped copper(II) clusters, with more or less complicated bridging systems, have already been reported, but they were obtained only through the use of exogenous bases or by oxidation of related Cu(I) derivatives.[2b,d,5a−c,h,k,n,o] At variance to that, in the case of **A**, the deprotonation of water and pyrazole to give OH^- and pz^- moieties is simply achieved by exploiting the basicity of acetate ions. Moreover, the formation of a trinuclear triangular cluster seems to take place only with pyrazole. As a matter of fact, reactions of copper(II) acetate with substituted azoles, namely, 4-MepzH, 3,5-Me_2pzH, 3,4,5-Me_3pzH, 3-Me-4-PhpzH, and 3-Me-5-PhpzH, yield mono- or dinuclear copper complexes where azoles coordinate the metal(s) only as neutral moieties.[7] A further key point concerns the carboxylate basicity; as a matter of fact, the

(3) (a) Yaghi, O. M.; Li, H.; Davis, C.; Richardson, D.; Groy, T. L. *Acc. Chem. Res.* **1998**, *31*, 474. (b) Eddaudi, M.; Moler, D. B.; Li, H.; Chen, B.; Reineke, T. M.; O'Keeffe, M.; Yaghi, O. M. *Acc. Chem. Res.* **2001**, *34*, 319. (c) Moulton, B.; Zaworotko, M. J. *Chem. Rev.* **2001**, *101*, 1629. (d) James, S. L. *Chem. Soc. Rev.* **2003**, *32*, 276. (e) Chen, B.; Fronczek, F. R.; Maverick, A. W. *Inorg. Chem.* **2004**, *43*, 8209. (f) Murugavel, R.; Walawalkar, M. G.; Dan, M.; Roesky, H. W.; Rao. C. N. R. *Acc. Chem. Res.* **2004**, *37*, 763. (g) Kubota, Y.; Takata, M.; Matsuda, R.; Kitaura, R.; Kitagawa, S.; Kato, K.; Sakata, M.; Kobayashi, T. C. *Angew. Chem., Int. Ed. Engl.* **2005**, *44*, 920. (h) Brandão, P.; Almeida Paz, F. A.; Rocha, J. *Chem. Commun.* **2005**, 171.

(4) (a) Huber, R. *Angew. Chem., Int. Ed.* **1989**, *28*, 848. (b) Messerschmidt, A.; Ressi, A.; Ladenstein, R.; Huber, R.; Bolognesi, M.; Gatti, G.; Marchesini, A.; Finazzi-Agro, A. *J. Mol. Biol.* **1989**, *206*, 513. (c) Messerschmidt, A.; Huber, R. *Eur. J. Biochem.* **1990**, *187*, 341. (d) Nguyen, H. H. T.; Shiemke, A. K.; Jacobs, A. J.; Hales, B. J.; Linstrom, M. E.; Chan, S. I. *J. Biol. Chem.* **1994**, *269*, 14995. (e) Suzuki, S.; Kataoka, K.; Yamaguchi, K. *Acc. Chem. Res.* **2000**, *33*, 728.

(5) (a) Hulsbergen, F. B.; ten Hoedt, R. W. M.; Verschoor, G. C.; Reedijk, J.; Spek, A. L. *J. Chem. Soc., Dalton Trans.* **1983**, 539. (b) Angaroni, M.; Ardizzoia, G. A.; Beringhelli, T.; La Monica, G.; Gatteschi, D.; Masciocchi, N.; Moret, M. *J. Chem. Soc., Dalton Trans.* **1990**, 3305. (c) Sakai, K.; Yamada, Y.; Tsubomura, T.; Yabuki, M.; Yamaguchi, M. *Inorg. Chem.* **1996**, *35*, 542. (d) Cole, A. P.; Root, D. E.; Mukherjee, P.; Solomon, E. I.; Stack, T. D. P. *Science* **1996**, *273*, 1848. (e) Jones, P. L.; Jeffery, J. C.; Maher, J. P.; McCleverty, J. A.; Rieger, P. H.; Ward, M. D. *Inorg. Chem.* **1997**, *36*, 3088. (f) Root, D. E.; Henson, M. J.; Machonkin, T.; Mukherjee, P.; Stack, T. D. P.; Solomon, E. I. *J. Am. Chem. Soc.* **1998**, *120*, 4982. (g) Setsune, J.-i.; Yokoyama, T.; Muraoka, S.; Huang, H.-w.; Sakurai, T. *Angew. Chem., Int. Ed.* **2000**, *39*, 1115. (h) Angaridis, P. A.; Baran, P.; Boča, R.; Cervantes-Lee, F.; Haase, W.; Mezei, G.; Raptis, R. G.; Werner, R. *Inorg. Chem.* **2002**, *41*, 2219. (i) Sanmartìn, J.; Bermejo, M. R.; Garcìa-Deibe, A. M.; Nascimento, O. R.; Lezama, L.; Rojo, T. *J. Chem. Soc., Dalton Trans.* **2002**, 1030. (j) López-Sandoval, H.; Contreras, R.; Escuer, A.; Vicente, R.; Bernès, S.; Nöth, H.; Leigh, G. J.; Barba-Behrens, N. *J. Chem. Soc., Dalton Trans.* **2002**, 2648. (k) Boča, R.; Diháň, L'.; Mezei G.; Ortiz-Pérez, T.; Raptis, R. G.; Telser, J. *Inorg. Chem.* **2003**, *42*, 5801. (l) Dong, G.; Chun-qi, Q.; Chun-ying, D.; Keliang, P.; Qing-jin, M. *Inorg. Chem.* **2003**, *42*, 2024. (m) Shen, W.-Z.; Yi, L.; Cheng, P.; Yan, S.-P.; Liao, D. Z.; Jiang, A.-H. *Inorg. Chem. Commun.* **2004**, *7*, 819. (n) Mezei, G.; Raptis, R. G. *Inorg. Chim. Acta* **2004**, *357*, 3279. (o) Mezei, G.; Rivera-Carrillo, M.; Raptis, R. G. *Inorg. Chim. Acta* **2004**, *357*, 3721.

(6) Monari, M.; Pandolfo, L.; Pettinari, C. 7° FIGIPS Meeting in Inorganic Chemistry, Lisbon, June 11−14; 2003, p 323.

(7) Casarin, M.; Corvaja, C.; di Nicola, C.; Falcomer, D.; Franco, L.; Monari, M.; Pandolfo, L.; Pettinari, C.; Piccinelli, F.; Tagliatesta, P. *Inorg. Chem.* **2004**, *43*, 5865.

reaction of Hpz with copper(II) trifluoroacetate leads only to the formation of the mononuclear derivative $[Cu(CF_3COO)_2(Hpz)_2]$.[7]

To rationalize these preliminary findings, we decided to test the reactivity of Hpz with different copper(II) carboxylates, checking the role played by steric effects (different lengths and shapes) of carboxylate chains in the synthesis of trinuclear triangular copper(II) clusters and in their assemblies into supramolecular arrangements. The most relevant results of this study are herein reported. Briefly, by reacting copper(II) formate, propionate, and butyrate with Hpz, three neutral trinuclear triangular complexes (hereafter **1**, **2**, and **3**, respectively) characterized by the presence of $[Cu_3(\mu_3\text{-}OH)(\mu\text{-}pz)_3(RCOO)_2]$ moieties (R = H, CH_3CH_2, $CH_3CH_2CH_2$) have been obtained. Despite the analogies present in compounds **1**−**3**, X-ray crystal structure determinations evidenced different supramolecular assemblies. Particularly, 1D coordination polymers (**1**) and hexanuclear "islands" (**2** and **3**), formed through the coupling of trinuclear triangular clusters, have been observed. In **2**, the hexanuclear islands are further connected through 12-membered rings to generate a 1D coordination polymer. Re-examination of the solid-state structure of the previously reported compound **A**[7] revealed the presence of 28-membered rings, interacting to form a 2D coordination polymer. Copper(II) formate, propionate, and butyrate react with 3,5-dimethylpyrazole (Hpz*), yielding compounds **4**−**6** where the azole is coordinated exclusively as a neutral molecule, analogously to what is observed with copper(II) acetate.[7] Solid-state and solution electronic spectra, ESI mass spectra, room-temperature magnetic susceptibility measurements, variable-temperature EPR experiments, and theoretical density-functional (DF) calculations have also been performed on **1**−**3**.

Experimental Section

Material and Methods. All chemicals were purchased from Aldrich and used without further purification. The synthesis and recrystallization of compounds **1**−**6**, as well as of copper(II) propionate and butyrate, were carried out in the air. Elemental analyses (C, H, N) were performed with a Fisons Instruments 1108 CHNS-O elemental analyzer. IR spectra were recorded from 4000 to 100 cm^{-1} with a Perkin-Elmer System 2000 FT-IR instrument. The electrical conductivities of methanol solutions were measured with a Crison CDTM 522 conductimeter at room temperature. Positive electrospray mass spectra were obtained with a Series 1100 MSI detector HP spectrometer, using MeOH as the mobile phase. Solutions for electrospray ionization mass spectrometry (ESI-MS) were prepared using reagent-grade methanol, and obtained data (masses and intensities) were compared to those calculated by using the IsoPro isotopic abundance simulator, version 2.1.[8] Peaks containing copper(II) ions were identified as the centers of isotopic clusters. The magnetic susceptibilities were measured at room temperature (20−28 °C) by the Gouy method with a Sherwood Scientific Magnetic Balance MSB-Auto, using $HgCo(NCS)_4$ as calibrant, and were corrected for diamagnetism with the appropriate Pascal constants. The magnetic moments (in BM) were calculated from the equation $\mu_{eff} = 2.84(X_m^{corr}T)^{1/2}$. The EPR spectra were recorded with a Bruker ER 200 X-band spectrometer equipped with a nitrogen flow variable-temperature system for measurements in the range 110−350 K. Solid-state and solution UV−vis spectra were recorded on a Varian Cary 5E spectrophotometer equipped with a device for reflectance measurements.

Computational Details. Density-functional (DF) calculations have been carried out by using the ADF 2002 package.[9] Optimized geometries have been evaluated by employing generalized gradient corrections self-consistently included through the Becke−Perdew formula.[10] A triple-ζ Slater-type basis set has been used for i) Cu atoms, ii) all the atoms directly bonded to the Cu atoms, and iii) the hydroxyl and pyrazole H atoms, whereas a double-ζ basis set has been adopted for the remaining atoms of the complexes. The inner cores of Cu (1s2s2p), O (1s), C (1s), and N (1s) atoms have been kept frozen throughout the calculations. All of the numerical experiments have been carried out by including spin−polarization effects. Information about the localization and the bonding/antibonding character of selected MOs over a broad energy range has been obtained by referring to density of states (DOS) and partial DOS (PDOS). Corresponding curves have been computed by weighting one-electron energy levels by their basis orbital percentage and by applying a 0.25 eV Lorentzian broadening.

Syntheses. Copper(II) propionate and butyrate were prepared following a previously reported procedure[11] that was slightly modified. As an example, the synthesis of copper(II) propionate is indicated below.

Wet basic copper carbonate, freshly prepared from 10 g of $CuSO_4 \cdot 5H_2O$ (40 mmol) and K_2CO_3, was transferred, in small portions, into a stirred solution of 12 g of propionic acid (160 mmol) in 200 mL of water. The solid dissolved, forming a blue-green solution that was stirred for 24 h until the effervescence ceased. The solution was filtered, concentrated under vacuum to 120 mL, and then allowed to evaporate in the air. Deep-green, large crystals were formed and separated, washed with 2 portions of 5 mL of cold water, dried under vacuum, washed with 3 portions of diethyl ether, and further dried under vacuum at 40 °C in the presence of solid KOH. This procedure appears to eliminate crystallization water, thus yielding anhydrous copper(II) propionate (6.1 g, 72% based on starting copper sulfate).

Copper(II) butyrate was prepared analogously, obtaining tiny, well-formed, green-blue crystals (yield 63%).

The use, in the previous syntheses, of commercial, dry, basic copper carbonate resulted in slightly lower yields of copper(II) carboxylates.

$[Cu_3(\mu_3\text{-}OH)(\mu\text{-}pz)_3(HCOO)_2(Hpz)_2]$, 1. Hydrated copper(II) formate (3.22 g, 14.27 mmol) was dissolved in 30 mL of water. To the light blue solution was added a Hpz solution (1.79 g, 26.29 mmol) in 10 mL of water under stirring. After 5 min, a dark blue solid started to precipitate. The suspension was stirred for 12 h, and then the solid was filtered off, washed with 10 mL of water, and dried under vacuum (yield 0.85 g, 27%). Mother liquors were allowed to evaporate in the air, yielding an additional 1.47 g of a less pure compound **1**. By carrying out the reaction in ethanol, the recovered yield was 81%. Recrystallization by slow evaporation in the air of an EtOH solution of **1** yielded well formed crystals, suitable for an X-ray crystal structure determination, containing one

(8) Senko, M. W. *IsoPro Isotopic Abundance Simulator*, version 2.1; National High Magnetic Field Laboratory, Los Alamos National Laboratory: Los Alamos, NM, 1994.

(9) *Amsterdam Density Functional Package*, version 2002; Vrjie Universiteit: Amsterdam, The Netherlands, 2002.

(10) (a) Becke, A. D. *Phys. Rev. A* **1988**, *38*, 3098. (b) Perdew, J. P. *Phys. Rev. B* **1986**, *33*, 8822.

(11) Martin, R. L.; Waterman, H. *J. Chem. Soc.* **1957**, 2545.

molecule of crystallization water per molecule of **1** (see X-ray Crystallography).

1. Mp: 170 °C dec. Anal. Calcd for $C_{17}H_{22}N_{10}O_6Cu_3$(**1**·$H_2O$): C, 31.26; H, 3.39; N, 21.54. Found: C, 31.00; H, 2.87; N, 21.28. IR (Nujol, cm^{-1}): 3607 (m), 3330 (br), 3140 (sh), 3124 (m), 2600 (br, NH, OH, CH), 1628 (s), 1606 (s), 1566 (s), 1488 (m), 1407 (m), 1377 (sh, CO), 452 (br), 356 (s), 321 (w), 301 (w), 280 (w), 265 (w, Cu−O, Cu−N). ESI-MS (+) (MeOH) (higher peaks, relative abundance %): 454 (30) $[Cu_3(OH)(pz)_3(HCOO)]^+$, 476 (65) $[Cu_3(OH)_2(pz)_3(MeOH)(H_2O)]^+$, 504 (85) $[Cu_3(OH)(pz)_3(HCOO)(MeOH)(H_2O)]^+$, 526 (65) $[Cu_3(OH)_2(pz)_3(MeOH)_2(H_2O)_2]^+$, 536 (100) $[Cu_3(OH)(pz)_3(HCOO)(MeOH)_2(H_2O)]^+$, 572 (60) $[Cu_3(OH)(pz)_3(HCOO)(Hpz)(MeOH)(H_2O)]^+$, 629 (33) $[Cu_3(OH)(pz)_3(HCOO)(Hpz)(MeOH)(H_2O)]^+$, 697 (33) $[Cu_4(OH)(pz)_4(HCOO)_2(Hpz)]^+$, 981 (43) $[Cu_6(OH)(pz)_6(HCOO)_4]^+$. μ_{eff} (296 K): 2.187 μ_B. Λ_M (EtOH, 1×10^{-4} M): 31.5 Ω^{-1} mol^2 cm^{-1}. λ_{max}/nm (reflectance): 610, 647. λ_{max}/nm (3.64×10^{-3} M MeOH solution): 627 ($\epsilon = 155$).

$[Cu_3(\mu_3\text{-}OH)(\mu\text{-}pz)_3(CH_3CH_2COO)_2(EtOH)]$, 2. Copper(II) propionate (1.935 g, 9.2 mmol) was dissolved in 30 mL of ethanol and 2 mL of water, and a solution of Hpz (0.643 g, 9.45 mmol) in 20 mL of ethanol was added under stirring. The obtained dark blue solution was stirred for 10 min and allowed to stay overnight, yielding a blue powder that was filtered, washed with 5 mL of ethanol, and dried under vacuum (yield 1.225 g, 66%). Mother liquors were concentrated in the air yielding an additional 0.155 g of a less pure compound. In mother liquors, propionic acid was detected. The solid was recrystallized by slow evaporation of a diluted ethanol solution, yielding deep blue, well-formed crystals of **2** suitable for an X-ray crystal structure determination.

2. Mp: 273−274 °C. Anal. Calcd for $C_{17}H_{26}N_6O_6Cu_3$: C, 33.97; H, 4.36; N, 13.98. Found: C, 33.20; H, 4.38; N, 13.59. IR (Nujol, cm^{-1}): 3627 (m), 3418 (br), 3137 (w), 3117 (w, OH, CH), 1661 (m), 1609 (m), 1547 (s), 1491 (m), 1433 (m), 1417 (m), 1378 (m, CO), 509 (s), 480 (br), 456 (br), 367 (s), 325 (w), 280 (w, Cu−O, Cu−N). ESI-MS (+) (MeOH) (higher peaks, relative abundance %): 496 (10) $[Cu_3(OH)_2(pz)_2(C_2H_5COO)(MeOH)_2]^+$, 538 (18) $[Cu_3(pz)_3(C_2H_5COO)_2]^+$, 570 (15) $[Cu_3(pz)_3(C_2H_5COO)_2(MeOH)]^+$, 606 (28) $[Cu_3(pz)_3(C_2H_5COO)_2(H_2O)_2(MeOH)]^+$, 657 (50) $[Cu_4(OH)_3(pz)_2(C_2H_5COO)_2(H_2O)_4]^+$, 1029 (55) $[Cu_6(OH)_3(pz)_7(C_2H_5COO)(H_2O)_3]^+$, 1065 (100) $[Cu_6(OH)_3(C_3H_3N_2)_7(C_2H_5COO)(H_2O)_5]^+$. μ_{eff} (296 K): 2.264 μ_B. Λ_M (EtOH, 1×10^{-4} M): 14.0 Ω^{-1} mol^2 cm^{-1}. λ_{max}/nm (reflectance): 611, 655. λ_{max}/nm (1.61×10^{-3} M MeOH solution): 614 ($\epsilon = 210$).

$[Cu_3(\mu_3\text{-}OH)(\mu\text{-}pz)_3(CH_3(CH_2)_2COO)_2(MeOH)(H_2O)]$, 3. Copper(II) butyrate (0.821 g, 3.45 mmol) was dissolved in 70 mL of water, and a solution of Hpz (0.265 g, 3.89 mmol) in 5 mL of water was added under stirring, obtaining a dark blue solution from which a blue solid started to precipitate after a few minutes. The suspension was stirred overnight and filtered, obtaining a solid that was washed with 5 mL of water and dried under vacuum (yield 0.452 g). Butyric acid was detected in the mother liquors. The solid was recrystallized by slow evaporation in the air of a methanol solution, yielding deep blue crystals of **3** suitable for an X-ray crystal structure determination.

3. Mp: 241−243 °C. Anal. Calcd for $C_{18}H_{30}N_6O_7Cu_3$: C, 34.15; H, 4.78; N, 13.28. Found: C, 34.85; H, 4.05; N, 14.07. IR (Nujol, cm^{-1}): 3144 (w), 3124 (w), 2800 (br, OH, CH), 1570 (s), 1540 (s), 1491 (m), 1436 (s), 1397 (s), 1377 (m, CO), 500 (s), 474 (s), 377 (s), 368 (s), 326 (m), 306 (w), 279 (w), 245 (m, Cu−O, Cu−N). ESI-MS (+) (MeOH) (higher peaks, relative abundance %): 496 (20) $[Cu_3(OH)(pz)_3(C_3H_7COO)]^+$, 546 (67) $[Cu_3(OH)(pz)_3(C_3H_7COO)(MeOH)(H_2O)]^+$, 566 (67) $[Cu_3(pz)_3(C_3H_7COO)_2]^+$, 578 (50) $[Cu_3(OH)(pz)_3(C_3H_7COO)(MeOH)_2(H_2O)]^+$, 598 (55) $[Cu_3(pz)_3(C_3H_7COO)_2(MeOH)]^+$, 634 (100) $[Cu_3(OH)(pz)_3(C_3H_7COO)_2(MeOH)(H_2O)+H]^+$, 671 (62) $[Cu_4(OH)_4(pz)_2(C_3H_7COO)(MeOH)_4]^+$, 1071 (75) $[Cu_6(OH)_3(pz)_7(C_3H_7COO)(MeOH)_2(H_2O)]^+$. μ_{eff} (296 K): 2.654 μ_B. Λ_M (EtOH, 1×10^{-4} M): 13.4 Ω^{-1} mol^2 cm^{-1}. λ_{max}/nm (reflectance): 611, 654. λ_{max}/nm (1.20×10^{-3} M MeOH solution): 610 ($\epsilon = 242$).

$[Cu(HCOO)_2(Hpz^*)_2]$, 4. Hydrated copper(II) formate (3.22 g, 14.27 mmol) was dissolved in 20 mL of ethanol. To the light blue solution was added a Hpz* solution (2.74 g, 28.5 mmol in 20 mL of ethanol) under stirring. After 30 min, 40 mL of light petroleum (40−60 °C) was added and the solution was refluxed for 2 h. A pale blue precipitate formed, and the suspension was stirred for 12 h. Then, the solid was filtered off, washed with 10 mL of petroleum ether, and dried under vacuum (yield 4.84 g, 98%).

4. Mp: 134−137 °C. Anal. Calcd for $C_{12}H_{18}N_4O_4Cu$: C, 41.68; H, 5.25; N, 16.20. Found: C, 41.53; H, 5.45; N, 16.43. IR (Nujol, cm^{-1}): 3169 (br), 3110 (w), 3076 (w), 3025 (w, NH, CH), 1650 (s), 1613 (s), 1573 (sh), 1557 (sh), 1493 (s, CO), 439 (m), 368 (m), 324 (m), 303 (w), 277 (m), 243 (w, Cu−O, Cu−N). ESI-MS (+) (MeOH) (higher peaks, relative abundance %): 97 (20) $[pz^*H_2]^+$, 254 (100) $[Cu(pz)(pz^*H)]^+$. μ_{eff} (296 K): 1.81 μ_B. Λ_M (EtOH, 1×10^{-4} M): 25 Ω^{-1} mol^2 cm^{-1}.

$[Cu(CH_3CH_2COO)_2(Hpz^*)_2]$, 5. Copper(II) propionate (1.935 g, 9.2 mmol) was dissolved in 20 mL of diethyl ether. To the blue solution was added a Hpz* solution (1.78 g, 18.5 mmol in 20 mL of diethyl ether) under stirring. After 1 h, 50 mL of light petroleum (40−60 °C) was added and the solution was refluxed for 6 h. A pale blue precipitate formed, and the suspension was stirred for 12 h. Then, the solid was filtered off, washed with 10 mL of petroleum ether, and dried under vacuum (yield 2.95 g, 80%).

5. Mp: 112−113 °C. Anal. Calcd for $C_{16}H_{26}N_4O_4Cu$: C, 47.81; H, 6.52; N, 13.94. Found: C, 47.72; H, 6.85; N, 14.21. IR (Nujol, cm^{-1}): 3179 (m), 3115 (m), 3086 (m), 3025 (m, NH, CH), 1556 (s), 1421 (s, CO), 530 (br), 430 (w), 350 (w), 326 (sh), 322 (sh), 314 (s), 277 (w), 265 (br, Cu−O, Cu−N). ESI-MS (+) (MeOH) (higher peaks, relative abundance %): 97 (100) $[pz^*H_2]^+$, 328 (43) $[Cu(CH_3CH_2COO)(pz^*)_2]^+$. μ_{eff} (296 K): 1.82 μ_B. Λ_M (EtOH, 1×10^{-4} M): 14 Ω^{-1} mol^2 cm^{-1}.

$[Cu(CH_3(CH_2)_2COO)_2(Hpz^*)_2]$, 6. Copper(II) butyrate (1.64 g, 7.9 mmol) was dissolved in 100 mL of diethyl ether. To the blue solution was added a Hpz* solution (1.78 g, 18.5 mmol in 20 mL of diethyl ether) under stirring. After 2 h, 100 mL of light petroleum (40−60 °C) was added and the solution was refluxed for 12 h. The solution was then cooled and allowed to stay overnight, yielding a pale blue powder that was filtered, washed with 25 mL of petroleum ether, and dried under vacuum (yield 1.82 g, 54%).

6. Mp: 98−101 °C. Anal. Calcd for $C_{18}H_{30}N_4O_4Cu$: C, 50.28; H, 7.03; N, 13.03. Found: C, 50.11; H, 7.28; N, 13.31. IR (Nujol, cm^{-1}): 3182 (m), 3118 (m), 3087 (m), 3029 (m, NH, CH), 1553, 1420 (CO), 593 (br), 506 (s), 431 (m), 369 (sh), 360 (s), 313 (sh), 310 (sh), 306 (s), 299 (s, Cu−O, Cu−N). ESI-MS (+) (MeOH) (higher peaks, relative abundance %): 97 (10) $[pz^*H_2]^+$, 342 (100) $[Cu(CH_3(CH_2)_2COO)(pz^*)_2]^+$. μ_{eff} (296 K): 1.86 μ_B. Λ_M (EtOH, 1×10^{-4} M): 13 Ω^{-1} mol^2 cm^{-1}.

X-ray Crystallography. The X-ray intensity data for **1**, **2**, and **3** were measured on a Bruker AXS SMART 2000 diffractometer equipped with a CCD detector. Cell dimensions and the orientation matrix were initially determined from a least-squares refinement on reflections measured in three sets of 20 exposures, collected in three different ω regions, and eventually refined against all data. For all crystals, a full sphere of reciprocal space was scanned by 0.3° ω steps, with the detector kept at 5.0 cm from the sample.

Table 1. Crystal Data and Experimental Details for **1·H$_2$O**, **2**, and **3**

compound	**1·H$_2$O**	**2**	**3**
formula	$C_{17}H_{22}Cu_3N_{10}O_6$	$C_{17}H_{26}Cu_3N_6O_6$	$C_{18}H_{30}Cu_3N_6O_7$
fw	653.07	601.06	633.10
T (K)	293(2)	293(2)	293(2)
λ (Å)	0.71073	0.71073	0.71073
cryst syst	monoclinic	triclinic	triclinic
space group	$P2_1$	$P\bar{1}$	$P\bar{1}$
a (Å)	7.7544(2)	10.3056(4)	10.380(1)
b (Å)	16.9830(4)	10.7908(4)	11.471(1)
c (Å)	9.0732(2)	11.2778(4)	11.953(1)
α (deg)	90	99.1881(9)	98.536(3)
β (deg)	97.9980(10)	114.4869(8)	113.362(2)
γ (deg)	90	90.8244(9)	99.324(3)
cell vol (Å^3)	1183.25(5)	1122.17(7)	1253.3(2)
Z	2	2	2
Dc (Mg m^{-3})	1.833	1.779	1.678
μ(Mo Kα) (mm^{-1})	2.728	2.863	2.571
F(000)	658	610	646
cryst size (mm)	0.12 × 0.20 × 0.25	0.20 × 0.25 × 0.30	0.15 × 0.23 × 0.33
θ limits (deg)	2.27−30.02	1.92−30.02	1.85−29.99
reflns collected	15519 ($\pm h$, $\pm k$, $\pm l$)	14726 ($\pm h$, $\pm k$, $\pm l$)	16409 ($\pm h$, $\pm k$, $\pm l$)
unique observed reflns [$Fo > 4\sigma(Fo)$]	6814 ($R_{int} = 0.0351$)	6535 ($R_{int} = 0.0292$)	7244 ($R_{int} = 0.0691$)
GOF on F^2	0.985	1.026	0.985
R1 (F),[a] wR2 (F^2)[b]	0.0321, 0.0740	0.0287, 0.0748	0.0548, 0.1339
largest diff peak and hole (e Å^{-3})	0.629 and −0.402	0.471 and −0.416	1.704 and −0.672

[a] $R1 = \sum||Fo| - |Fc||/\sum|Fo|$. [b] $wR2 = [\sum w(Fo^2 - Fc^2)^2/\sum w(Fo^2)^2]^{1/2}$, where $w = 1/[\sigma^2(Fo^2) + (aP)^2 + bP]$, and where $P = (Fo^2 + 2Fc^2)/3$.

The software SMART[12] was used for collecting frames of data, indexing reflections, and determination of lattice parameters. The collected frames were then processed for integration by the SAINT program,[12] and an empirical absorption correction was applied using SADABS.[13] The structures were solved by direct methods (SIR 97)[14] and subsequent Fourier syntheses and refined by full-matrix least-squares on F^2 (SHELXTL)[15] using anisotropic thermal parameters for all non-hydrogen atoms. All hydrogen atoms, except the pyrazole and hydroxy hydrogens which were located in the Fourier map and refined isotropically, were added in calculated positions, included in the final stage of refinement with isotropic thermal parameters, $U(H) = 1.2U_{eq}(C)$ [$U(H) = 1.5U_{eq}(C-Me)$], and allowed to ride on their carrier carbons. For complex **1**, the absolute configuration was determined (Flack parameter 0.04(1)). One molecule of crystallization water was found in the asymmetric unit of **1**. Crystal data and details of data collection for compounds **1**−**3** are reported in Table 1.

Results and Discussion

The reaction of copper(II) formate, propionate, and butyrate with Hpz in water or ethanol (Scheme 2[16]) generates, in fairly good yields, neutral trinuclear triangular copper(II) derivatives **1**−**3** having the general formula [$Cu_3(\mu_3$-OH)(μ-pz)$_3$(RCOO)$_2$L$_x$L′$_y$], analogously to what was previously observed in the synthesis of compound **A**.[7]

All three compounds are dark blue solids, barely soluble in water and alcohols, with the exception of **1** which easily dissolves in MeOH. Compounds **2** and **3** are slightly soluble in dichloromethane, and **3** is also slightly soluble in acetone. The characterizations of **1**−**3** were carried out through conventional methods. More specifically, positive ESI mass spectra of methanol solutions are consistent with the existence of trinuclear structures and, in the cases of compounds **2** and **3**, significant signals attributable to hexanuclear species are also well evident (see Experimental Section). Conductivities measurements (ethanol solution) indicate, for compounds **1**−**3**, a partial ionic dissociation to trinuclear cationic units and anionic carboxylates. In accord with ESI-MS and X-ray data, dissociation is larger in the case of the formate derivative **1** (which is also the species having the greater solubility), likely because of weaker Cu−O$_{(formate)}$ bonding interactions (vide infra). The IR spectrum of **1** shows two similar sets of strong bands corresponding to ν_{as}(COO) (1606 and 1566 cm^{-1}) and ν_s(COO) (1410 and 1407 cm^{-1}). The $\Delta\nu$ values [ν_{as}(COO) − ν_s(COO)] are in accordance with a nearly symmetric bridging bidentate coordination of carboxylates.[17] The IR spectrum of **2** is characterized by a different profile: two sets of absorptions of very different intensities, due to carboxylates, are actually present. The former, weak, set exhibits a $\Delta\nu$ of ca. 176 cm^{-1} and could be assigned to a propionate, symmetrically bridging two Cu(II) centers; the latter set has a $\Delta\nu$ of ca. 130 cm^{-1}, typical of a bidentate nonsymmetric coordination. Once again, the

Scheme 2

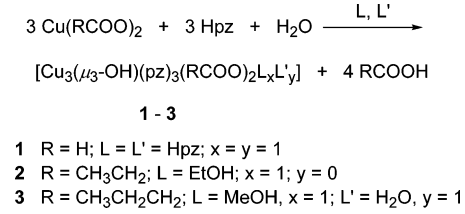

(12) *SMART & SAINT Software Reference Manuals*, version 5.051 (Windows NT Version); Bruker Analytical X-ray Instruments, Inc.: Madison, WI, 1998.
(13) Sheldrick, G. M. *SADABS Program for Empirical Absorption Correction*; University of Göttingen: Göttingen, Germany, 1996.
(14) Altomare, A.; Cascarano, G.; Giacovazzo, C.; Guagliardi, A.; Moliterni, A. G. G.; Burla, M. C.; Polidori, G.; Camalli, M.; Siliqi, D. *Acta Crystallogr., Sect. A* **1996**, *52*, C79.
(15) Sheldrick, G. M. *SHELXTL Plus (Windows NT Version) Structure Determination Package*, Version 5.1; Bruker Analytical X-ray Instruments, Inc.: Madison, WI, 1998.
(16) In Scheme 2, in the case of compound **3**, the product obtained after recrystallization in methanol is indicated.
(17) Deacon, G. B.; Phillips, R. J. *Coord. Chem. Rev.* **1980**, *33*, 227.

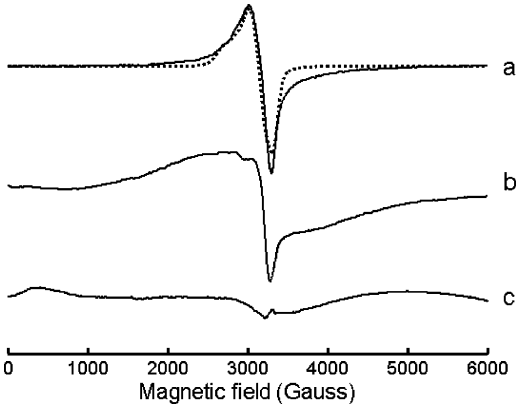

Figure 1. EPR powder spectra at $T = 110$ *K* of **1** (a), **2** (b), and **3** (c). The dotted line is the spectral simulation of the spectrum of **1**. The three experimental spectra are vertically shifted for clarity. They have been recorded with the same experimental parameters and are reported on the same vertical scale.

IR spectrum of **3** exhibits two sets of absorptions characterized by a $\Delta\nu$ of ca. 140 cm^{-1}, in accordance with the nonsymmetric bridging coordination of a butyrate ion.[18] Room-temperature magnetic susceptibility values of **1**−**3** range between 2.187 and 2.654 μ_B for each trinuclear unit. They are lower than those expected for three independent copper(II) ions, indicating some kind of exchange coupling, in accordance to what was previously observed for compound **A**.[7]

Because of the low solubility of compounds **1**−**3**, we could not obtain their EPR spectra in solution. However, we succeeded in recording them for powder samples. The spectra recorded at the temperature of 120 K are reported in Figure 1.

The spectrum of **1** is shown with its simulation, calculated by assuming a doublet species ($S = 1/2$) and a rhombic **g** tensor whose principal values, $\mathbf{g}_1 = 2.03$, $\mathbf{g}_2 = 2.16$, and $\mathbf{g}_3 = 2.37$, are typical of a doublet state copper complex. Weak broader features at the wings of the doublet spectrum are also visible and cannot be reproduced by considering only a doublet species. Spectra of **1** in the range 100−350 K show a decrease of the doublet spectrum intensity by increasing *T*, following a Curie law, whereas the broad part of the spectrum shows an opposite behavior. The possible explanation of these findings is that the broad spectrum can be related to a higher spin state, possibly a quartet state, generated by spin coupling within trinuclear units, becoming thermally populated at higher temperatures. The temperature dependence evidences an antiferromagnetic coupling, as is frequently obtained in trinuclear clusters.

The EPR spectrum of **2** also shows a doublet pattern in the magnetic field range 2500−3500 G; nevertheless, a strong broad band, extending over the full magnetic field sweep, is also present. The spectrum of **3** is weak and broad, and the narrow doublet feature is almost absent. Despite the structureless line shape of the broad spectra of **2** and **3** that prevents any meaningful simulation, it is possible to assess that their wideness is certainly related to high-spin species ($S > 1/2$) whose spin relaxation is sufficiently fast to broaden lines and to decrease their intensity not only at room temperature but also at 120 K.

An interpretation of different EPR behaviors of **1**−**3** can be proposed by referring to their structures, which are determined from X-ray diffraction experiments carried out on single crystals obtained by slow evaporation of diluted water or alcohol solutions.

The structures of **1**−**3** are all characterized by the presence of the $[Cu_3(\mu_3\text{-OH})(\mu\text{-pz})_3]^{2+}$ core and two carboxylate ions; different neutral molecules complete the coordination sphere of the Cu(II) centers. In all three compounds, the central μ_3-OH capping ions are placed only slightly out of the planes defined by the three Cu(II) ions (0.565(2) (**1**), 0.421(1) (**2**), and 0.551(3) Å (**3**)), a feature common to this kind of compound.[2b,d,5a−c,h,k,n,o,7] Despite these similarities, there are significant differences in the ligand arrangements around the metal centers and in the solid-state intermolecular interactions, thus originating diverse molecular architectures.

The molecular structures of compounds **1**−**3** are shown in Figure 2a−c, and their relevant bond lengths and angles are reported in Table 2.

In **1** (see Figure 2a), unlike **2**, **3** (vide infra), and the previously reported complex **A**,[7] the two formate ligands are bound to the same copper atom, Cu(1), whereas both Cu(2) and Cu(3) are coordinated by one terminal pyrazole pointing away from the capping hydroxy group. The coordination geometry at Cu(1) is distorted square pyramidal, with one oxygen of the formate group, O(2), occupying an axial position and another oxygen, O(4), belonging to the second formate group in an equatorial site. The two $Cu-O_{(carboxylate)}$ distances Cu(1)−O(4) = 2.029(2) and Cu(1)−O(2) = 2.304(2) Å are nonequivalent. Even the Cu(2) center has a distorted square pyramidal environment, with the apical position occupied by a formate oxygen belonging to another trinuclear unit (Cu(2)−O(3′) = 2.436(2) Å). The third copper atom, Cu(3), has a square planar geometry, with a bound pyrazole having the nitrogen hydrogen on the same side of the μ_3-OH group, opposite to the orientation of the pyrazole coordinated to Cu(2).

Complex **2** (see Figure 2b) differs from **1** by the coordination of the propionate ligands to two copper centers and by the presence of an ethanol molecule coordinated to the third copper center. The coordination geometry at Cu(2) is distorted square pyramidal, with the oxygen O(6) of the ethanol in the apical position (Cu(2)−O(6) = 2.358(1)), and three equatorial sites are occupied by two nitrogens of two bridging pyrazolates and the oxygen of the μ_3-OH group. The last equatorial position is occupied by an oxygen, O(3′), of a third propionate ion belonging to another trinuclear unit and acting as a bridge in a monodentate fashion (Cu(2)−O(3′) = 2.003(1) Å). Even the coordination at the Cu(3) center is distorted square pyramidal, with one oxygen, O(4), of the propionate ligand occupying an equatorial site and the symmetry equivalent oxygen, O(4″), of another trinuclear unit in the axial position. A square planar geometry is instead

(18) Nakamoto, K. Application in Organometallic Chemistry. *Infrared and Raman Spectra of Inorganic and Coordination Compounds*, 5th ed.; Wiley-Interscience: New York, 1997; p 271.

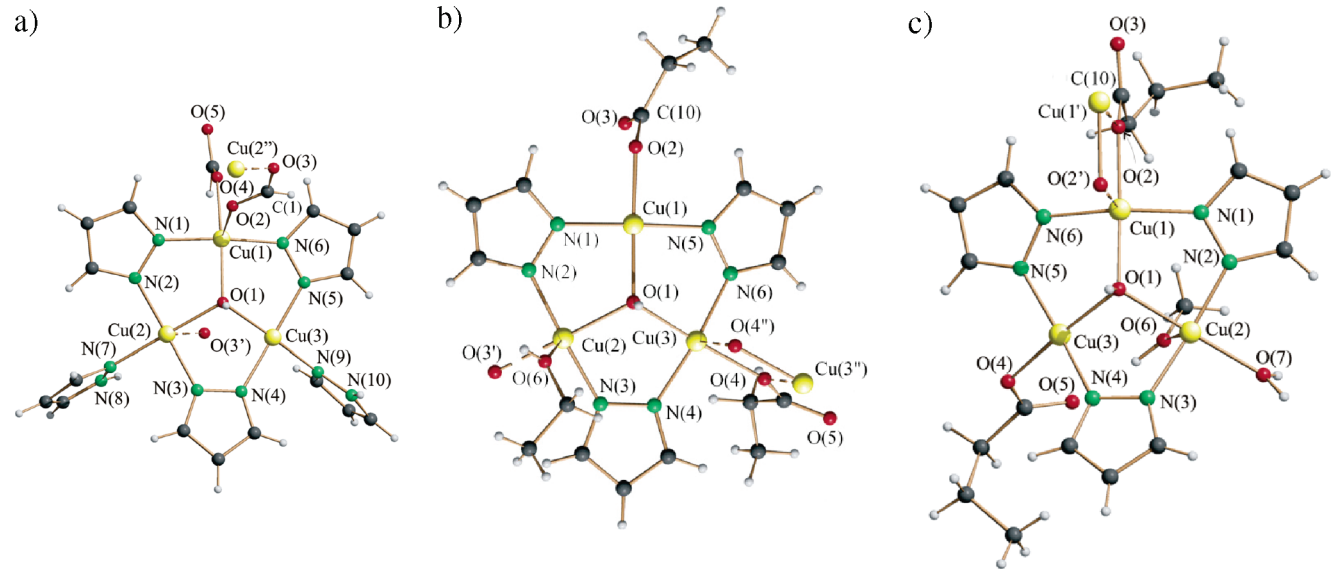

Figure 2. Molecular structures of **1**−**3** showing the coordination sphere of the Cu atoms. (a) In **1**, the dashed lines indicate the Cu−O bonds with two adjacent trinuclear units. Symmetry code: (I) $x + 1, y, z$; (II) $x - 1, y, z$. (b) In **2**, the dashed lines indicate the Cu−O bonds with two adjacent trinuclear units. Symmetry code: (I) $-x + 2, -y + 1, -z + 1$; (II) $-x + 1, -y + 1, -z$. (c) In **3**, the dashed lines indicate the Cu−O bonds with another trinuclear unit of **3**. Symmetry code: (I) $-x, -y, -z$.

Table 2. Selected Bond Lengths (Å) and Angles (deg)

Compound [**1**]·H_2O			
Cu(1)−O(1)	2.006(2)	Cu(3)−N(5)	1.950(3)
Cu(2)−O(1)	2.000(2)	Cu(3)−N(9)	2.024(3)
Cu(3)−O(1)	2.003(2)	Cu(2)−O(3′)	2.436(2)
Cu(1)−N(1)	1.939(2)	Cu(1)−O(2)	2.304(2)
Cu(1)−N(6)	1.941(2)	Cu(1)−O(4)	2.029(2)
Cu(2)−N(2)	1.962(3)		
Cu(2)−N(3)	1.950(3)	Cu(1)−O(1)−Cu(2)	113.22(9)
Cu(2)−N(7)	2.014(3)	Cu(1)−O(1)−Cu(3)	115.62(9)
Cu(3)−N(4)	1.951(3)	Cu(2)−O(1)−Cu(3)	108.24(9)
symmetry code	(I) $x + 1, y, z$		
Compound **2**			
Cu(1)−O(1)	1.980(1)	Cu(1)−O(2)	1.969(1)
Cu(2)−O(1)	1.999(1)	Cu(2)−O(3′)	2.003(1)
Cu(3)−O(1)	2.007(1)	Cu(2)−O(6)	2.358(1)
Cu(1)−N(1)	1.929(1)	Cu(3)−O(4)	1.993(1)
Cu(1)−N(5)	1.941(2)	Cu(3)−O(4″)	2.415(1)
Cu(2)−N(2)	1.943(1)		
Cu(2)−N(3)	1.946(2)	Cu(1)−O(1)−Cu(2)	115.61(6)
Cu(3)−N(4)	1.940(2)	Cu(1)−O(1)−Cu(3)	116.00(6)
Cu(3)−N(6)	1.946(2)	Cu(2)−O(1)−Cu(3)	115.43(6)
symmetry code	(I) $-x + 2, -y + 1, -z + 1$; (II) $-x + 1, -y + 1, -z$		
Compound **3**			
Cu(1)−O(1)	1.980(2)	Cu(1)−O(2′)	2.399(3)
Cu(2)−O(1)	2.007(2)	Cu(3)−N(5)	1.922(3)
Cu(3)−O(1)	1.988(3)	Cu(2)−O(6)	2.342(3)
Cu(1)−N(1)	1.948(3)	Cu(2)−O(7)	2.029(3)
Cu(1)−N(6)	1.947(3)	Cu(3)−O(4)	1.949(3)
Cu(2)−N(2)	1.937(3)		
Cu(2)−N(3)	1.950(3)	Cu(1)−O(1)−Cu(2)	117.2(1)
Cu(3)−N(4)	1.923(3)	Cu(1)−O(1)−Cu(3)	114.5(1)
Cu(1)−O(2)	1.986(3)	Cu(2)−O(1)−Cu(3)	106.2(1)
symmetry code	(I) $-x, -y, -z$		

present at Cu(1), which bears, as a terminal ligand, the second propionate anion bound through O(2) to the metal.

As already mentioned, the molecular structure of complex **3** (see Figure 2c) is more similar to those of **2** and **A**[7] than to that of **1**. In fact, the butyrate anions are coordinated to two different copper atoms, Cu(1) and Cu(3), but interestingly, one molecule of methanol and one molecule of water are bound to Cu(2). The coordination polyhedra of Cu(1) and Cu(2) are distorted square pyramids. Four stronger interactions around Cu(1) (Cu(1)−N(1) = 1.948, Cu(1)−N(6) = 1.947(3), Cu(1)−O(1) = 1.980(2), and Cu(1)−O(2)(butyrate) = 1.986(2) Å) define the base, and the weakly bonding apical interaction is established with the same butyrate oxygen, O(2′), that belongs to an adjacent unit related by inversion (Cu(1)−O(2′) = 2.399(3) Å). In the case of Cu(2), the square pyramidal geometry exhibits the methanol oxygen O(6) in the axial site and the water O(7) is in an equatorial position (Cu(2)−O(7) = 2.029(3) and Cu(2)−O(6) = 2.342(3) Å). Cu(3) is truly tetracoordinate in a slightly distorted square planar arrangement and bears a monodentate butyrate ligand, O(4).

In the crystals of **1**−**3** a significant contribution stabilizing the overall structural buildings, due to intermolecular $Cu-O_{(carboxylate)}$ interactions, is established and leads to the formation of coordination polymers. As a matter of fact, taking into account only the relatively stronger $Cu-O_{(carboxylate)}$ intermolecular interactions, namely those shorter than 2.5 Å, some interesting features, sketched in Chart 2, can be observed.

We start with the description of intermolecular interactions in compound **3**. Its crystal packing (Figure 3) can be rationalized in terms of centrosymmetric pairs of trinuclear molecules held together by O(2) (belonging to the carboxylate O(3)C(10)O(2) grouping), which doubly bridges the Cu(1)···Cu(1′) vector (two monatomic bridges of the type indicated in Chart 1f). These interactions generate hexanuclear islands, no longer connected to each other, that pile up along the *a* axis and establish hydrogen bonds among the uncoordinated carboxylate O(5) and the hydroxy groups O(6) (methanol) and O(7) (water).

Similar hexanuclear clusters can also be observed in the crystal packing of complex **2** (Figure 4). Analogously to **3**, they are formed through a four-membered ring constituted by two propionates asymmetrically bridging the Cu(3)···Cu(3′)

Chart 2. Sketches of Intermolecular Assemblies in **1**−**3**[a]

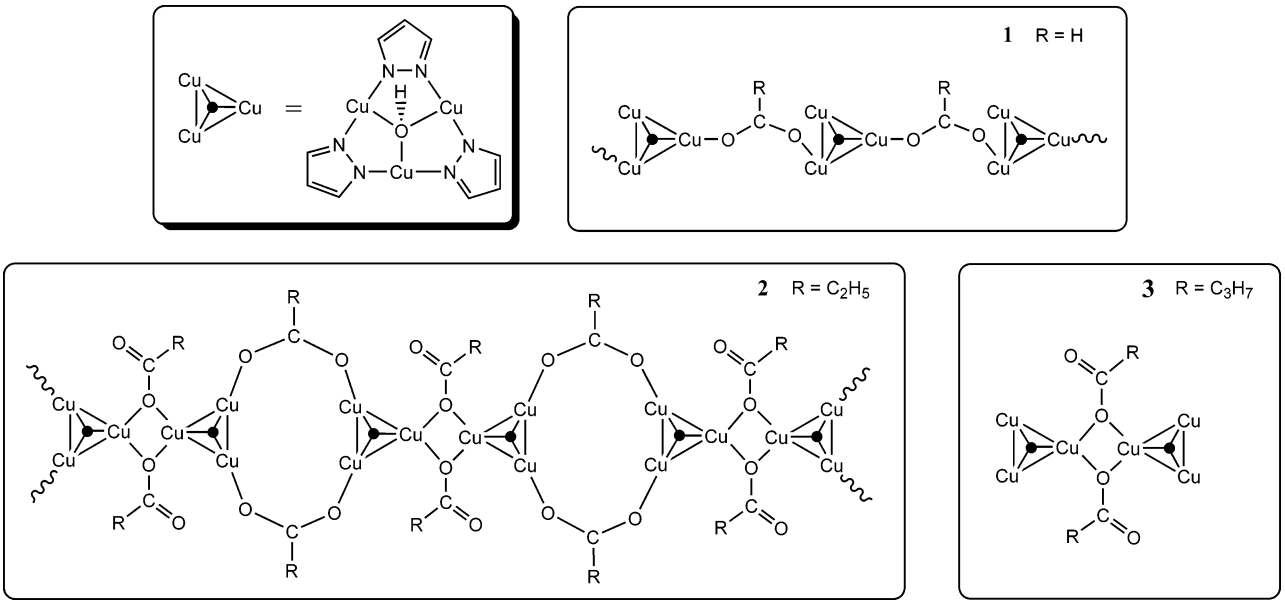

[a] Neutral ligands bonded to Cu(II) ions (Hpz, H_2O, MeOH, and EtOH) are omitted. Only carboxylate ions involved in intermolecular Cu−$O_{(carboxylate)}$ interactions shorter than 2.5 Å are sketched. Dots in the center of triangles indicate capping μ_3-OH.

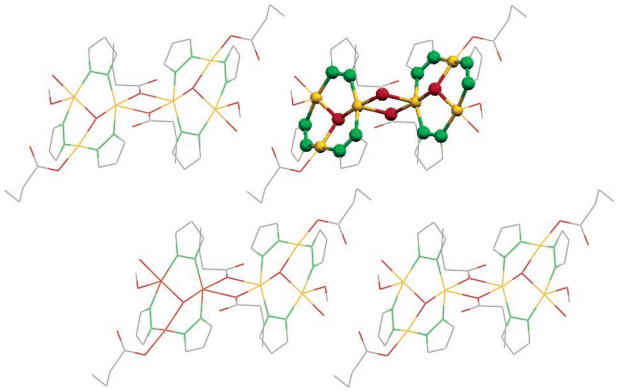

Figure 3. Arbitrary view of the crystal packing of **3** showing the hexanuclear island motifs (one of them is evidenced through ball-and-stick representation) that run along the *ab* diagonal. Hydrogen atoms are not shown. Color codes: red (oxygen), yellow (copper), green (nitrogen), gray (carbon).

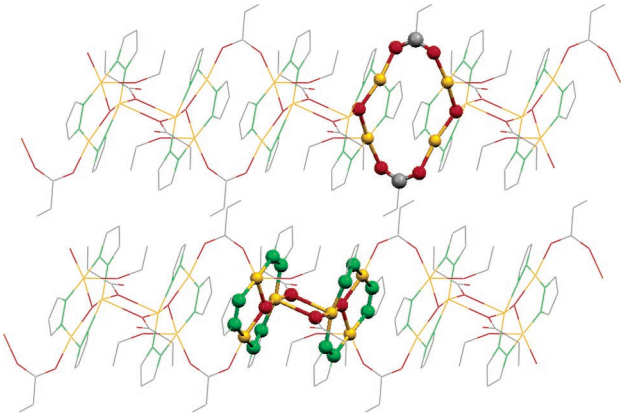

Figure 4. Crystal packing of **2**. View down the *c* axis showing two 1D polymeric frameworks. The 12-membered macrocycle (up) and the hexanuclear cluster (down) are highlighted by ball-and-stick representations. Hydrogen atoms are not shown. Color codes: red (oxygen), yellow (copper), green (nitrogen), gray (carbon).

vector (Cu(3)−O(4″) = 2.415(1) and Cu(3)−O(4) = 1.993(1) Å, respectively), but they are further linked to each other through two single syn−syn carboxylate bridges (Cu(1)−O(2)−C(10)−O(3)−Cu(2′) and Cu(1′)−O(2′)−C(10′)−O(3′)−Cu(2)) (Chart 1c), thus forming 12-membered rings and 1D coordination polymers.

Hexanuclear clusters are also present in the previously reported compound **A**.[7] They are strongly connected to each other (Cu−$O_{(carboxylate)}$ distances shorter than 2.5 Å) in a complicated way based on the coordination of acetate ions in a bridging syn−syn and monatomic bridging mode (Chart 1g) strictly related to the well-known connections between dinuclear units in several polymeric copper(II) carboxylates (Chart 1h).[19]

This arrangement generates 28-membered macrocycles (Chart 3) that can be considered as tertiary building units (TBU) self-assembling to form a 2D MOF. In Figure 5a, four of such TBUs are sketched and one of them is evidenced by space filling. The whole arrangement is not planar and can be better described as a corrugated sheet. The overall crystal structure of **A** is built up by a series of these parallel waved layers (Figure 5b).

Hexanuclear clusters are absent in **1**. Its crystal packing (Figure 6) shows that each trinuclear unit makes primarily intermolecular interactions with two neighbors through the oxygens of one bidentate formate ligand (Cu(1)−O(2)−C(1)−O(3)−Cu(2″) bridging in the syn−anti way as shown in Chart 1d), thus generating a polymeric 1D zigzag ribbon running along the *a* axis.[20] On the other hand, if we also

(19) (a) Mehrotra, C.; Bohra, R. C. *Metal Carboxylates*; Academic Press: New York, 1983. (b) Doedens, R. J. *Prog. Inorg. Chem.* **1976**, *21*, 209. (c) Melnik, M. *Coord. Chem. Rev.* **1982**, *42*, 259. (d) Kato, M. Y.; Muto, Y. *Coord. Chem. Rev.* **1988**, *92*, 45.

(20) A 1D coordination polymer structurally strictly related to **1** has been observed in the crystal packing of $[Cu_3(\mu_3\text{-OH})(\mu\text{-pz})_3(NO_3)_2(Hpz)_2]\cdot H_2O$,[5a] where the connections among trinuclear triangular clusters are provided by nitrate ions instead of $HCOO^-$. One molecule of crystallization water for each trinuclear unit is present in both compounds.

Chart 3. Schematic Representation of the 28-Membered Macrocycle Present in the Crystal Structure of **A**

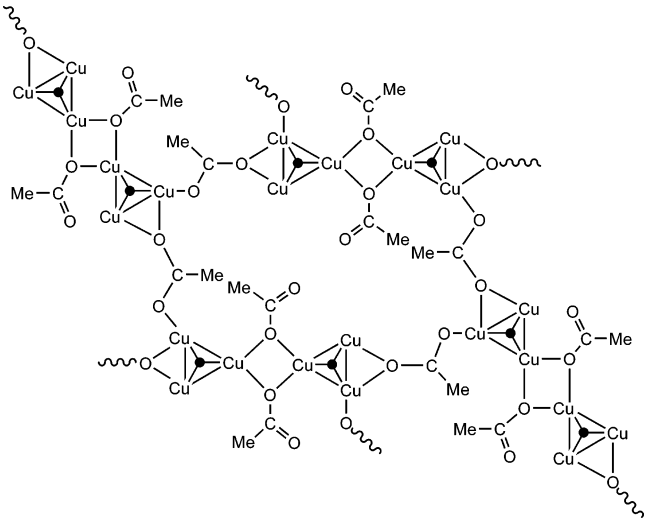

take into account weaker Cu−$O_{(carboxylate)}$ interactions, then a supramolecular 2D coordination polymer can be detected in **1** as well. As a matter of fact, adjacent 1D ribbons are connected to each other through the interactions of Cu(3) with O(5‴) (symmetry code (III) $-x, y + 0.5, -z + 1$) of the second formate ion of the adjacent chain at 2.773(3) Å. Incidentally, Cu(3) reaches an octahedral coordination through another weak interaction with O(3′), lying at ca. 2.75 Å on the opposite side with respect to O(5‴) (O(3′)−Cu(3)−O(5‴) = ca. 165°). Therefore, altogether, O(3) can be considered engaged only in two intermolecular interactions (vide infra) with one trinuclear unit. Taking these weak interactions into account, the 20-membered macrocycles (one of them is evidenced by space filling in Figure 6) form waved 2D fishing net-like coordination polymeric sheets. Similarly to **A**, a series of these parallel waved layers form the overall crystal structure of **1** (see Supporting Information).

In the analysis of the supramolecular assemblies of compounds **1**−**3** and **A**, we have concentrated our attention only on Cu−$O_{(carboxylate)}$ interactions, independently of their strength. On the other hand, we are perfectly aware that other important bonding features, such as relatively strong and weak hydrogen bonds, cooperate to stabilize trinuclear structures as well as to form the above indicated supramolecular 1D and 2D polymeric metal−organic frameworks.[21]

Also, the presence of different ancillary ligands in the trinuclear units could be of some relevance in determining the overall structures of **1**−**3**. In fact, in **1**, both formate ions are bonded to the same Cu ion, thus making it possible to coordinate two neutral pyrazole molecules to the other copper(II) ions of the trinuclear unit. In contrast to that, in **A**, **2**, and **3**, each carboxylate is bonded to a single Cu ion (in each trinuclear unit) and, only in the case of **A**, a single pyrazole molecule is coordinated to the third Cu(II), likely causing the strong distortion of the trinuclear unit.[7] In the case of **2** and **3**, it seems that there is not enough space for the coordination of a neutral pyrazole and only small molecules of solvent(s) coordinate to copper(II) ions. It is also noteworthy that these small coordinated molecules may play some role in the determination of the overall structure, as witnessed by the fact that, in the case of copper propionate, two other trinuclear triangular species having different neutral ancillary ligands have been observed.[22]

As previously mentioned, the structural features above-discussed provide a key to rationalize magnetic susceptibility data and the EPR results. Particularly, in **1**, trinuclear clusters can be seen as practically isolated units and the magnetism mainly results from the spin coupling within them. The antiferromagnetic coupling gives rise to a doublet ground state with a quartet state that is possibly thermally accessible at room temperature. A different result is observed when dealing with **2** and **3**, where two trinuclear clusters are strongly connected, forming hexanuclear units. More specifically, their higher magnetic moments and broader EPR spectra are related to the presence of high spin states, arising from unpaired spin coupling in hexanuclear units. The total spin of each of these units may range from singlet ($S = 0$) to septet ($S = 3$). The relative energy and population of these spin states depend on the intensity of pairwise exchange interactions between copper atoms in the hexanuclear unit. The broad and weak pattern of the EPR spectra of **2** and **3** is explained by a partial population of the singlet state (EPR silent) and by some contribution from higher spin states, whose spectra are broadened by fast-spin relaxation. The fact that the singlet state is the lowest-energy state points to an overall antiferromagnetic spin coupling within hexanuclear clusters.

MeOH solution and solid-state reflectance spectra of **1**−**3**, in the range 300−800 nm, are reported in Figure 7. Solid-state spectra (Figure 7, left) are very similar[23] and display two complex absorption bands in the ranges 300−400 and 500−700 nm. The former spectral feature consists of a broad band centered at ∼335 nm, and the latter is distinguished by two evident maxima positioned around 610 and 650 nm for all three compounds. Furthermore, the spectra are characterized by two shoulders around 520 and 740 nm. Spectral patterns are only slightly modified in solution (Figure 7, right), and besides the broadening of the absorption band at lower energies, the most intriguing feature is the appearance of an evident shoulder at ∼410 nm in **1** and at ∼360 nm in **2** and **3**.

Analogously to **A**,[7] insights into spectral features of **1**−**3** can be gained by referring to the outcomes of quantum mechanical calculations. ADF numerical experiments have been carried out for models of **1**, **2**, and **3** (hereafter $\mathbf{M}_1$, $\mathbf{M}_2$, and $\mathbf{M}_3$) by taking into account that a series of Cu−O bonds (hereafter Cu···O) between the metal atoms of a specific $Cu_3(\mu_3$-OH) core and carboxylate ligands directly bonded to the nearest $Cu_3(\mu_3$-OH) cores (see Chart 2) concur to determine the solid-state architecture of the title compounds. These interactions have been modeled by using the

(21) The analysis of these particular bonding features deserves a deeper examination and will be the subject of a forthcoming paper.

(22) Monari, M.; Pandolfo, L.; Pettinari, C. *Unpublished results*.

(23) It is noteworthy that the solid-state UV−vis spectra of **1**−**3** are almost identical to that of **A** (see ref 7).

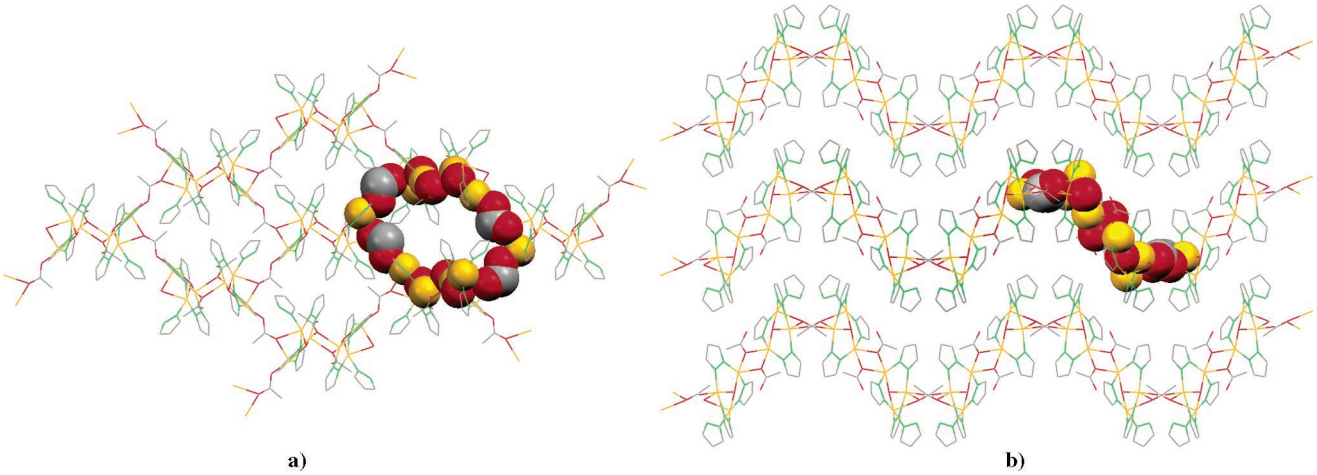

Figure 5. Crystal packing of **A**. (a) View down the *a* axis showing the 2D coordination polymer formed through the assembling of 28-membered macrocyclic TBUs. One of them is evidenced by space filling. (b) View down the *c* axis showing the parallel waved 2D polymeric sheets. Hydrogen atoms are not shown. Color codes: red (oxygen), yellow (copper), green (nitrogen), gray (carbon).

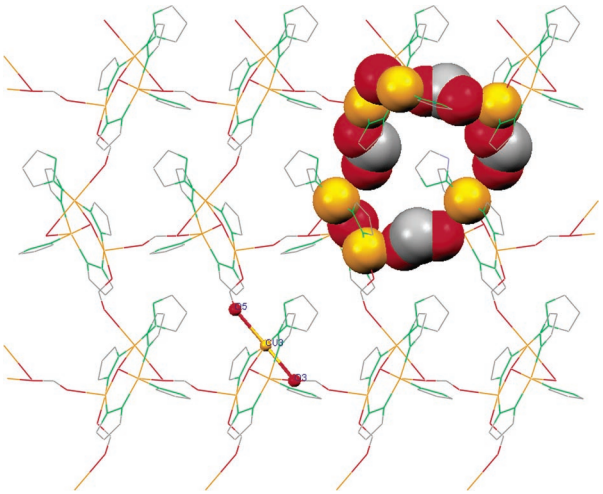

Figure 6. Crystal packing of **1**. View down the *c* axis. The zigzag 1D coordination polymer ribbons generate a 2D framework through Cu(3)···O(5) and Cu(3)···O(3) weak interactions (evidenced through ball-and-stick representation). One 20-membered macrocycle is evidenced by space filling. Crystallization water molecules and hydrogen atoms are not shown. Color codes: red (oxygen), yellow (copper), green (nitrogen), gray (carbon).

same procedure previously adopted to carry out ADF calculations for **A**.[7] More specifically, Cu···O bonds in **1** and **2** have been mimicked by replacing the corresponding formate/propionate groups with two molecules of formic/propionic acid whose atoms were placed in the same crystallographic positions occupied by formate/propionate ligands and by placing the acid H atoms at 0.99 Å from the O atoms along the original O−Cu directions. Thus, actual spin-polarized calculations have been run for the $[Cu_3(\mu_3\text{-}OH)(\mu\text{-}pz)_3(HCOO)_2(Hpz)_2](H_2O)(HCOOH)_2$ (**M**$_1$) and $[\{Cu_3(\mu_3\text{-}OH)(\mu\text{-}pz)_3(C_2H_5COO)_2(EtOH)\}_2](C_2H_5COOH)_2$ (**M**$_2$) model systems, while **M**$_3$ corresponds to the hexanuclear island $\{Cu_3(\mu_3\text{-}OH)(\mu\text{-}pz)_3(C_3H_7COO)_2(MeOH)(H_2O)\}_2$.

Now, before anything else, it needs to be emphasized i) that besides the important role certainly played by bridging pyrazolate ligands in determining the stability of trinuclear units of **1**−**3**, their spectroscopic and magnetic properties are mostly determined by the $Cu_3(\mu_3\text{-}OH)$ core[5k,7,24] and ii) that a first, qualitative description of the bonding scheme of the $Cu_3(\mu_3\text{-}OH)$ core, simply based on symmetry arguments, can be very helpful in rationalizing ADF results. As far as the latter point is concerned, the qualitative description of the electronic features of the $Cu_3(\mu_3\text{-}OH)$ core of **A**, where Cu centers all have a square pyramidal coordination, has been previously reported.[7] We are aware that cores of **1**−**3** include only two pentacoordinate Cu ions, and the third one has a square planar environment;[25] however, it is quite straightforward to show that the qualitative bonding scheme proposed for the core of **A** still holds for those of **1**−**3**. As a matter of fact, it is well-known[26] that the square pyramidal coordination lifts the 5-fold degeneracy of the Cu(II) d orbitals, giving rise to four ($b_2 + e + a_1$) low-lying MOs and a partially filled b_1 level. The assembly of three Cu(II) centers sharing the μ_3-OH ligand generates 30 ($3 \times 5 \times 2$) Cu-based spin-orbitals (SOs), 27 of them being occupied. Cu-based SOs can be further divided into two sets, α and β,[7] with the former including the linear combinations of ($b_2 + e + a_1$) MOs (24 low-lying SOs) and the latter being constituted by the linear combinations of the b_1-like level (6 high-lying SOs, 3 of them occupied). In the presence of a local C_3 axis, the β set spans the (a + e) representations, thus having the correct symmetry to interact with the occupied (a + e) OH^- frontier orbitals. The square planar coordination around Cu(3) in **1**, Cu(1) in **2**, and Cu(3) in **3** (collectively called Cu_x) stabilizes the corresponding a_1 d orbital, thus giving rise to a set of four closely spaced MOs (see Figure 2 in ref 27). At variance to that, the energy position of the fifth Cu_x d orbital (the singly occupied b_1 MO) is negligibly affected on passing from the square pyramidal coordination to the square planar one.[27] It is then easy to see that the partition of the $Cu_3(\mu_3\text{-}OH)$ core d orbitals in two sets of levels (α and β) (see Figure 8), with the former

(24) La Monica, G.; Ardizzoia, G. A. *Prog. Inorg. Chem.* **1997**, *46*, 151.
(25) Even if this is strictly true for **2** and **3**, the pentacoordination of Cu(3) in **1** involves a weakly bonded apical O(5) atom of an adjacent zigzag chain positioned at 2.772 Å from it.
(26) Rossi, A. R.; Hoffmann, R. *Inorg. Chem.* **1975**, *14*, 365.
(27) Hoffmann, R.; Chen, M. M. L.; Elian, M.; Rossi, A. R.; Mingos, D. M. P. *Inorg. Chem.* **1974**, *13*, 2666.

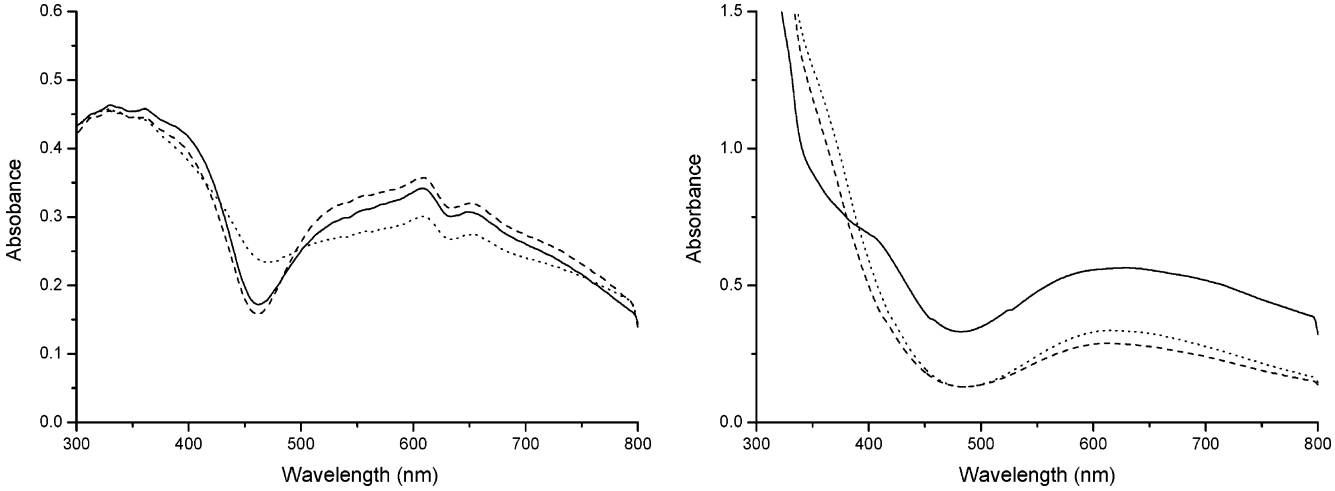

Figure 7. Solid-state reflectance (left) and MeOH solution (right) electronic spectra of **1** (solid lines), **2** (dotted lines), and **3** (dashed lines).

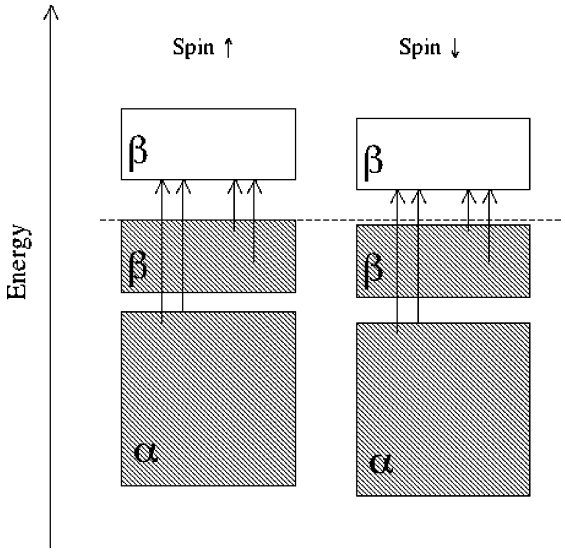

Figure 8. Qualitative outline of the Cu-based energy levels corresponding to the spin ↑ and spin ↓ components of the $Cu_3(\mu_3\text{-OH})$ core. Dashed patterns include occupied energy levels. White patterns include empty energy levels. Electronic transitions from β levels and outermost α levels to the LUMO are also sketched.

including 24 low-lying SOs and the latter being constituted by the linear combinations of the b_1-like level (6 high-lying SOs, 3 of them occupied), is still effective in **1**−**3**.

In discussing the analysis of ADF results, it is interesting to point out that, despite the already mentioned different coordinative arrangements of Cu(II) ions in **1**−**3** and **A**, Cu Hirshfeld gross atomic charges[28] as well as Cu_3 3d PDOS of $\mathbf{M}_1$−$\mathbf{M}_3$ are very similar along the series (see Supporting Information**)**. On the basis of this, we propose to assign the spectral features of **1**−**3** by referring to our assignments of the UV−vis spectrum of **A**.[7] According to that, the complex absorption band extending from 500 to 700 nm can be ascribed either to transitions between occupied and empty SOs belonging to the β set or to transitions between the topmost lying SOs of the α set and unoccupied levels of the β set. Interestingly, the energy difference between the LUMO and the maximum of the Cu_3 3d PDOS amounts to ∼3 eV, thus allowing us to assign the broad band lying between 300 and 400 nm to electronic excitations from the "bulk" of the α set to empty levels of the β set.

To investigate the influence of the pyrazole substituents on the formation of triangular trinuclear Cu(II) clusters and their possible supramolecular assembly, we have also performed the reaction of the copper(II) formate, propionate, and butyrate with 3,5-dimethylpyrazole (Hpz*). In all cases, the formation of 1:2 $Cu(RCOO)_2$/Hpz* adducts was observed (**4**, R = H; **5**, R = CH_3CH_2; **6**, R = $CH_3(CH_2)_2$). These compounds were characterized through elemental analysis, IR spectroscopy, ESI-MS, room-temperature magnetic susceptibility, and EtOH solution conductivity.

The $\Delta\nu$ criterion[17] suggests that $RCOO^-$ in **4**−**6** behave as bidentate bridging ligands, likely determining a binuclear cage structure as in $[Cu_2(CH_3COO)_4(H_2O)_2]$[29] or polymeric zigzag chains as in $[Cu(CF_3COO)_2(Hpz)_2]$.[7] Some medium bands at ca. 290 cm^{-1}, absent in the spectra of the starting Cu(II) carboxylates, can be tentatively assigned to Cu−N stretchings.[30] The positive ESI mass spectra of methanol solutions of compounds **5** and **6** show the most intense signals as clusters exactly simulated by $[Cu(RCOO)(Hpz^*)_2]^+$. Few other signals, deriving from the free ligand Hpz*, are present. The most intense signal of the ESI-MS of **4** corresponds to the cluster $[Cu(pz^*)(Hpz^*)]^+$. Such evidence agrees with the ionic dissociation of the formate ligand and deprotonation of Hpz* in solution, which have been confirmed by conductivity measurements and the easy detection of formic acid. As a matter of fact, conductivity values in solution for compounds **4**−**6** are of the same order-of-magnitude as those reported for **1**−**3**, the formate **4** being the more dissociated species. Magnetic susceptibility data pertaining to **4**−**6** are in the range expected (1.81−1.86 μ_B) for paramagnetic mononuclear Cu(II) species.

(28) Hirshfeld charges of Cu(1), Cu(2), and Cu(3) are 0.43, 0.38, and 0.37, respectively, in **1**; 0.44, 0.41, and 0.43, respectively, in **2**; 0.42, 0.45, and 0.41, respectively, in **3**; and 0.41, 0.41, and 0.39, respectively, in **A** (for the last compound see ref 7).

(29) van Niekerk, J. N.; Schoening, F. R. L. *Acta Crystallogr., Sect. C* **1953**, *6*, 227.

(30) Yang, Y.-Y.; Shi, Q.; Shi, Q.-Z.; Gao, Y.-C.; Zhou, Z.-Y. *Polyhedron* **1999**, *18*, 2009.

A careful examination of compounds **4**−**6** has not allowed us to unambiguously characterize them as mono-, di-, or polynuclear structures. On the other hand, by using our synthetic procedure, we obtained the sole formation of compounds presenting a $Cu(RCOO)_2$/Hpz* ratio of 1:2, where the azole coordinates to copper(II) as a neutral ligand. Trinuclear $[Cu_3(\mu_3\text{-}OH)(\mu\text{-}pz^*)_3(RCOO)_2L_x]$ clusters were not obtained, and this fact seems to indicate that the deprotonation of substituted azoles by carboxylate ions does not occur or that its extent is not sufficient to drive the reaction toward the self-assembling in trinuclear triangular units (see also ref 7).

Conclusions

Through this study, we have shown that neutral μ_3-OH capped trinuclear triangular copper pyrazolate complexes can be obtained simply by reacting pyrazole with copper(II) carboxylates in the presence of water, thus confirming a behavior previously observed with copper(II) acetate.[7]

A fundamental fact is that both Cu(II) carboxylates and unsubstituted pyrazole are necessary to obtain triangular clusters because the reactions follow different paths if different Cu(II) salts or substituted pyrazoles are employed. Certainly, the intrinsic basicity of carboxylate ions plays a leading role in the deprotonation of both pyrazole and water to give the coordinating fragments pyrazolate and OH^-, respectively, but it is likely that the templating effect of carboxylate ions is also important. Even the absence of substituents on pyrazole is a determinant factor, but it is questionable if this is related to their steric hindrance. As a matter of fact, i) the formation of trinuclear triangular derivatives was not observed when 4-methylpyrazole was employed[7] (a methyl in that position is expected to have insignificant steric effects) and ii) μ_3-OH capped Cu_3 derivatives having bridging cumbersome L^- ligands have been actually synthesized.[2b,d,5b,c,h,k,n,o] On the other hand, in the latter cases, the result was achieved by employing exogenous bases to generate OH^- and L^- ions in suitable concentrations.

A second, likely most relevant, observation is related to the self-assembling of triangular units to yield coordination polymers. Most of the Cu(II) ions in **1**−**3** and **A** show a square pyramidal pentacoordination[31] that is reached because of the coordination of neutral fragments, namely, Hpz, H_2O, MeOH, or EtOH, or through the formation of carboxylates bridges. The latter are responsible for the self-assembling of trinuclear SBUs to originate stable coordination polymers with different supramolecular structures, spanning from 1D in **1** to hexanuclear units in **2**, **3**, and **A**. In **2**, hexanuclear clusters are further linked together to yield 12-membered cycles, thus giving rise to a 1D coordination polymer, whereas in **A**, they self-assemble in a more different way, leading to the formation of 28-membered macrocycles, that, as sort of tertiary building units, self-generate an extended 2D MOF. It is noteworthy that almost all the interactions involving carboxylate bridges binding trinuclear SBUs in **1**−**3** and **A** are relatively strong, having $Cu-O_{(carboxylate)}$ distances in the range 1.97−2.44 Å.

In light of these data, even though further experimental work is certainly needed, it seems reasonable to predict a similar behavior, at least, with other copper(II) carboxylates having saturated or unsaturated chains. It is also evident that the formation of different MOFs, through the assembly of triangular trinuclear SBUs as well as their possible porosity,[32] are related to the steric differences among carboxylates.

Finally, the existence of trinuclear cores in solution is supported by the results of ESI-MS spectra and by the analogies between solid-state and corresponding solution UV−vis spectra. Moreover, solid-state spectra of **1**−**3** (and **A**, too[7]) in the range 300−800 nm are almost identical. These data suggest that ESI-MS and UV−vis spectroscopy may be potential tools to employ in the future to detect the existence of similar species in the absence of X-ray data.

In our laboratories, further work is in progress to test the behavior of Cu(II) and other transition-metal carboxylates (saturated and unsaturated) with Hpz in different reaction conditions. Also, the influence of neutral coordinating molecules (with or without the ability to be involved in hydrogen bonds and to promote supramolecular interactions to form organometallic porous frameworks) is currently under examination. We have also started a study on the reactivity and properties of these trinuclear clusters and their polymeric assemblies.

Acknowledgment. The authors thank Dr. Gregorio Bottaro (Istituto di Scienza e Tecnologie Molecolari-CNR Sez. Padova) for the registration of UV−vis spectra. The Universities of Bologna, Camerino, and Padova are gratefully acknowledged.

Supporting Information Available: X-ray crystallographic files in CIF format for the structures of **1**−**3**. Figures reporting Cu_3 3d PDOS of $\mathbf{M}_1$, $\mathbf{M}_2$, and $\mathbf{M}_3$ and crystal packing of **1** viewed down the *a* axis. This material is available free of charge via the Internet at http://pubs.acs.org.

IC050678L

(31) Cu(1) in **2** and Cu(3) in **3** present a slightly distorted square planar tetracoordination, whereas for Cu(3) in **1**, see Results and Discussion.

(32) The 28-membered macrocycles present in compound **A** form channels that are in large part obstructed by pyrazolate moieties (see Figure 7a). Possibly more interesting and, at the present, under examination are the interlayer voids present in the same compound (see Figure 7b).